

## Projected Changes in Mid-Twenty-First-Century Extreme Maximum Pavement Temperature in Canada

CHRISTOPHER G. FLETCHER, LINDSAY MATTHEWS, JEAN ANDREY, AND ADAM SAUNDERS

*Department of Geography and Environmental Management, University of Waterloo, Waterloo, Ontario, Canada*

(Manuscript received 26 August 2015, in final form 10 November 2015)

### ABSTRACT

Future climate warming is virtually certain to bring about an increase in the frequency of heat extremes. Highway design and pavement selection are based on a temperature regime that reflects the local climate zone. Increasing heat extremes could, therefore, shift some areas into a different performance grade (PG) for pavement, and more-heat-resistant materials are associated with increased infrastructure costs. This study combines observations, output from global climate models, and a statistical model to investigate changes in 20-yr return values of extreme maximum pavement temperature  $TP_{max}$ . From a multimodel range of simulated  $TP_{max}$ , future changes in PG are computed for 17 major Canadian cities. Relative to a 1981–2000 baseline, summertime Canada-wide warming of 1°–3°C is projected for 2041–70. As a result, climate change is likely to bring about profound changes to the spatial distribution of PG, with the severity of the changes directly linked to the severity of the projected warming. Even under weak simulated warming, an increase in PG is projected for greater Toronto, which is Canada's largest urban area; under moderate (strong) warming 7 of 17 (9 of 17) major cities exhibit an increase. The influence of model spatial resolution is evaluated by comparing the results from global climate models with output from a set of regional climate models focused on North America. With the exception of mountainous terrain in western Canada, spatial resolution is not a major determining factor for projections of future PG changes.


## 1. Introduction

The quality of transport infrastructure is a key determinant of performance in the transport sector; transport performance, in turn, is reflected in the vibrancy of regional and national economies. It is thus not surprising that trends in transport investments have been steadily upward over the past several decades. Road infrastructure, in particular, is attracting large investments, because global road travel is expected to “almost double between now and 2050” (Koerner and Dulac 2013).

The lifespan and state of repair of transportation assets are affected by a number of factors, including their original designs as well as traffic loads. Empirical studies also reveal that weather accounts for a significant fraction

of deterioration, even when infrastructure is designed and constructed to standard, taking into account local climatic conditions. The transportation community is increasingly questioning whether climatic risks are being adequately incorporated into asset design and management, given the ways in which climate change is expected to result in new norms and extremes in all parts of the world (Seneviratne et al. 2012).

Indeed, observed and projected increases in intense precipitation, sea levels, storm surges, and maximum temperatures have profound implications for transportation infrastructure. Of concern in many parts of the world are intense rainfall and storm events that lead to flooding, washouts, and travel disruptions, as has been observed in recent years (Jaroszweski et al. 2015; Karim et al. 2014; Regmi and Hanaoka 2011). Temperature is also an important weather variable, however, especially for paved infrastructure because these assets are designed for a specific temperature range. Materials that are used to construct roadways experience temperature fluctuations that lead to the contraction and expansion of material. Cold temperatures can lead to thermal cracking and increased development of potholes, and

 Denotes Open Access content.

*Corresponding author address:* Christopher G. Fletcher, Dept. of Geography and Environmental Management, University of Waterloo, 200 University Ave. West, Waterloo, ON N2L 3G1, Canada.  
E-mail: chris.fletcher@uwaterloo.ca

DOI: 10.1175/JAMC-D-15-0232.1

© 2016 American Meteorological Society

hot temperatures can lead to buckling, subsidence, and rutting (Meyer and Weigel 2011). The premature deterioration of transportation infrastructure as a result of temperature changes has been identified in numerous reports as a possible concern (Chai et al. 2014; Hayhoe et al. 2010; IPCC 2014; Mills et al. 2007, 2009), but to our knowledge no previous studies have sought to quantify and project the extent of the problem for Canada. Preliminary studies indicate that the costs of maintenance and repair may increase in light of climate change and that there may be a need to update construction standards for roads, notwithstanding the higher costs of adaptation measures (Hayhoe et al. 2010; IPCC 2014). Increased high-temperature extremes can have an impact on costs in two ways. First, failure to change the materials' specifications for roadways in areas expected to experience more heat extremes will lead to premature deterioration, with serious cost implications. Second, in situations in which materials' specifications are changed to reflect future climatic conditions, there may be a need for modified asphalts whereby polymers or other additives are needed. In this case, asphalt costs can be expected to increase by approximately 10% (J. Duval 2006, unpublished conference presentation; available online at <http://www.docfoc.com/benefits-of-modified-asphalts-john-duval-pe-oregon-asphalt-conference-march>).

Canada is a particularly appropriate country for exploring the implications of temperature change on paved road systems for multiple reasons: Canada has more than a million kilometers of (two-lane equivalent) roads, of which more than 40% are paved (Transport Canada 2014); the expansiveness of Canada and the geographic distribution of population centers is such that current systems experience a wide range of thermal conditions; temperature changes have already been observed (Vincent and Mekis 2006; Zhang et al. 2000); the professional-engineering community is engaged with the issue of climate change (Engineers Canada 2008); and extreme-deterioration events have already been associated with temperature extremes [e.g., on 22 July 2012, maximum air temperatures in Toronto, Ontario, Canada, reached a record-breaking high of 34.4°C, causing pavement to buckle on areas of the 401 highway, which is Canada's busiest highway (News Staff 2012)]. In addition, recent evidence shows that significant changes to summertime extreme-heat events are projected by the mid-twenty-first century across Canada (Jeong et al. 2016). The costs associated with the physical rehabilitation and maintenance work are of primary concern to maintenance authorities, but increases in secondary costs associated with vehicle operation, user delays, and accidents due to traffic interruptions or hazards are also possible (Mills et al. 2007).

It is important to study the impacts of climate change when planning transportation infrastructure and future services. Many of these infrastructures are built for long lifespans that will be exposed to a changing climate (Boyle et al. 2013; Peterson et al. 2008). Asphalt roads in Canada are built to have an estimated productive life of ~28 yr, and bridges have an estimated service life of ~43 yr (Gagnon et al. 2008). These are the expected mean service lives of transportation infrastructure, but the reality is that more than one-half of the road infrastructure in Canada has actually surpassed its designed life expectancy. In 2008, 57% of Canadian bridges and 53% of roads had exceeded their useful designed life (Gagnon et al. 2008). This fact means that more than one-half of the road design and construction that occurs today will still be in use into the 2050s. As such, there are substantial costs that will accrue if systems are not properly designed and managed (Koetse and Rietveld 2009; Mills et al. 2009).

The current study provides quantitative estimates of the implications of extreme high temperatures for designing paved infrastructure in Canada. Using data from climate model simulations for 2041–70 and statistical modeling, we project extreme summer pavement temperatures across Canada, focusing in particular on the 17 largest urban areas. We then produce a map of the spatial distribution of appropriate performance grades (PG) for asphalt cement mixes by midcentury, noting where differences exist from current practices. Section 2 describes the observational and model data and the statistical methods employed. Section 3 presents the PG projections for pavement, and section 4 explores the impact on those projections of using higher-resolution climate-model simulations. In section 5, we present our principal conclusions and a discussion of the broader implications of this work.

## 2. Data and methods

### a. Observational data

Data for daily maximum near-surface air temperature  $T_{\max}$  are taken from the 10 km  $\times$  10 km Australian National University Splines package (ANUSPLIN) daily temperature grids for Canada made available by Natural Resources Canada and documented in the literature (Hopkinson et al. 2011; Hutchinson et al. 2009; McKenney et al. 2011). The observational baseline period for this study is 1981–2000, which is chosen to overlap with the output from the climate models (see section 2b). The data analyzed are annual maxima of  $T_{\max}$ , one value per year, providing a sample size of 20 yr for each grid cell. Although this is a shorter duration than would be ideal, it should be sufficient to provide a

representative estimate of the variability of the present climate (Kharin et al. 2005). This is important because we employ a change-field method whereby it is assumed that climate variability remains constant in the future: our estimates of climate change are produced by adding offsets derived from climate-model output to the observational baseline values.

We emphasize that all analyses are conducted by using a gridded temperature product rather than by using either the raw output from weather stations or statistical downscaling techniques to interpolate the gridded data to point locations. The gridded data ensure spatial and temporal homogeneity across Canada, but one limitation is that our estimates of temperature extremes for cities are extracted from the grid cell(s) closest to the center of each city. As a result, these values are very likely to be conservative relative to station observations because the gridded data represent temperature averaged over each 10-km<sup>2</sup> grid cell. No adjustments to correct for the effects of urban heat islands have been applied to the gridded data (Hutchinson et al. 2009).

To provide climatological context, we begin by examining the frequency of occurrence of maximum daily pavement temperatures  $TP_{\max}$  for all days in the baseline period (see section 2d for the method used to convert  $T_{\max}$  to  $TP_{\max}$ ), extracted from 3 of the 17 major Canadian cities analyzed in this study: Vancouver, British Columbia; Winnipeg, Manitoba; and Toronto (see Table 2). Figure 1 reveals several characteristics shared by all three cities (and by the majority of other cities examined; not shown). All reveal a bimodal distribution of temperatures, which arises from contributions from the two shoulder seasons in spring and autumn. The months with the coldest  $TP_{\max}$  in each city are December and January, and the months with the highest  $TP_{\max}$  are July and August. The daily  $TP_{\max}$  values in the individual months are generally normally distributed, which reflects the variation in incoming solar radiation over the days in each month. The larger spread of the distributions at Winnipeg and Toronto reveals the more continental nature of the climates at these locations when compared with the moderate maritime climate of Vancouver. Regardless of geographic location, however, all three cities display summertime days of extreme heat that deviate substantially from the seasonal mean. The overall extreme maximum  $TP_{\max}$  occurred in June 1988 in Winnipeg, July 1988 in Toronto, and August 1991 in Vancouver, with the different months of occurrence possibly reflecting the influence of the seasonal lag time of the ocean on extreme heat in Vancouver.

### b. Climate models

We draw output data from climate-model simulations performed in conjunction with two large assessment

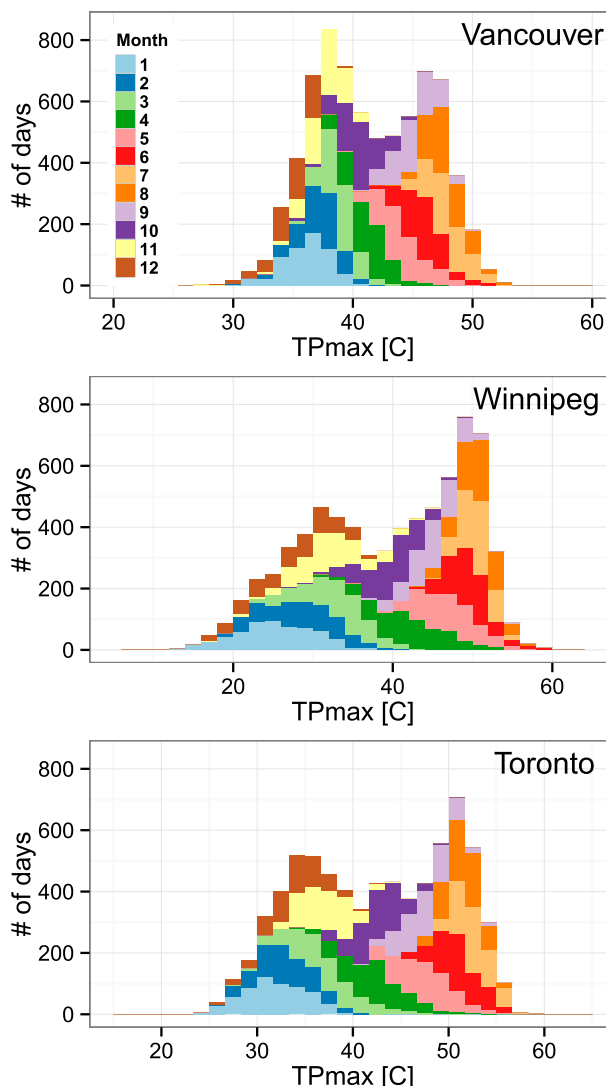


FIG. 1. Stacked histograms showing frequency of occurrence of daily  $TP_{\max}$ , color coded by month. Data are from ANUSPLIN observations for all years 1981–2000 and are extracted from the grid cell closest to the centers of (top) Vancouver, (middle) Winnipeg, and (bottom) Toronto. See Table 2 for latitude and longitude coordinates of each city.

projects. Daily  $T_{\max}$  values were retrieved from 10 general circulation model (GCM) simulations produced for phase 3 of the Coupled Model Intercomparison Project (CMIP3). For the period that overlaps with observations (1981–2000), we analyze output from the twentieth-century (historical) simulation “20C3M.” For the future period (2041–70), we use  $T_{\max}$  output from the Special Report on Emissions Scenarios (SRES) A2 scenario experiment, which corresponds to a business-as-usual carbon-dioxide emissions trajectory out to 2100 (Nakicenovic and Swart 2000). The models in this set of GCMs have typical spatial resolutions of 100–200 km<sup>2</sup>,

and they were considered state of the art when the simulations were produced around 2007; the output has been used in many studies of temperature extremes (Tebaldi et al. 2006). Significant model development has occurred since CMIP3, and a newer generation of models was more recently used to conduct a similar set of coordinated experiments for CMIP5. Published results show little change in the simulation of historical, or future, temperature extremes in CMIP5 in comparison with CMIP3 (Wuebbles et al. 2014), indicating that the projections are robust. Therefore, for brevity, we do not analyze CMIP5 data here.

In addition to the GCMs, we also include output from regional climate model (RCM) simulations, which was made available through the North American Regional Climate Change Assessment Project (NARCCAP; Mearns et al. 2009). RCMs are typically run at much higher spatial resolution than GCMs; for example, the NARCCAP models analyzed in this study have grid sizes of 25–40 km<sup>2</sup>. The trade-off is that the RCMs are limited-area models, meaning that their simulation domain is not global like the GCMs, but instead is restricted to one specific region of the globe. In the case of the NARCCAP RCMs the domain covers continental North America, including most of Canada, from approximately 25° to 70°N (Mearns et al. 2012). The RCMs are driven at the horizontal boundaries of this domain by input data extracted either from meteorological observations or from an existing GCM simulation. The NARCCAP RCMs are driven by observations for the baseline period 1981–2000 and by output from a suite of CMIP3 GCMs (including several of the same GCMs analyzed in this study; Table 1) following the same SRES A2 scenario for the future period of 2041–70. Within the RCM domain, the model operates just like a GCM, solving the governing equations and producing prognostic output for meteorological fields at daily frequency. This configuration means that, for areas within the RCM domain, we can directly compare the output from the RCMs and GCMs to assess the impact of horizontal resolution on projections of future temperature extremes. This comparison is of more than academic value: an ongoing discussion in the field concerns whether higher-resolution GCMs or a series of targeted RCM simulations offer better prospects for simulating regional climate changes (Jeong et al. 2016; Di Luca et al. 2012, 2013).

The time period selected for the future projections (2041–70) is aligned with the time segment simulated by each of the NARCCAP RCMs (unlike the GCMs, the RCMs were not run for the entire twenty-first century). This period is useful and relevant for the issue of highway infrastructure planning, since the typical lifetime for

TABLE 1. Code names of the GCMs and RCMs used in this study. The RCM names comprise the name of the RCM and, to the right of the underscore, the name of the GCM that was used to drive the RCM at its horizontal boundaries. The RCMs with driving GCMs that also appear in the list of GCMs are indicated with an asterisk. The two columns labeled  $\Delta T_{\text{JJA}}$  show, for each model, the summertime (JJA) mean near-surface air temperature change (°C) averaged across all of Canada for the 2041–70 period relative to 1981–2000. The last four rows show the multimodel mean  $\Delta T_{\text{JJA}}$ , as well as the 25th-, 50th-, and 75th-percentile values.

GCM name	$\Delta T_{\text{JJA}}$	RCM_GCM name	$\Delta T_{\text{JJA}}$
cccma_cgcm3_1	1.59	CRCM_ccsm	2.66
cnrm_cm3	1.85	CRCM_cgcm3*	2.33
csiro_mk3_0	1.08	ECP2_gfdl*	1.39
gfdl_cm2_1	1.29	HRM3_gfdl*	2.56
giss_model_e_r	1.60	HRM3_hadcm3	2.43
ipsl_cm4	3.37	MM5I_ccsm	1.58
miroc3_2_medres	2.73	RCM3_cgcm3*	2.26
miub_echo_g	2.26	RCM3_gfdl*	2.11
mpi_echam5	1.54	WRFG_ccsm	1.66
mri_cgcm2_3_2a	0.98	WRFG_cgcm3*	1.37
Mean	1.83	Mean	2.04
p25	1.36	p25	1.60
p50	1.60	p50	2.18
p75	2.16	p75	2.41

highway infrastructure is several decades. Therefore, planners acting today are already making decisions about pavement types whose implications reach into the future projection range. In addition, from a climatological perspective, GCM projections demonstrate that over North America the emergence of the signal of climate change from the background natural variability is highly unlikely before the mid-twenty-first century (Hawkins et al. 2014). Therefore, by delaying our analyses to cover 2041–70, we maximize the chances of observing a robust climate-change signal in the data while at the same time providing an analysis time frame that remains relevant to infrastructure planning, since newly constructed asphalt roads typically last 15–25 years without resurfacing and concrete lasts even longer.

### c. Statistical methods

We follow closely the methods for analysis of extreme values described in Coles (2001) and applied to temperature extremes by Kharin et al. (2005). A generalized extreme value (GEV) distribution is fit to the annual maxima of 7-day running-mean  $T_{\text{max}}$  at each gridpoint location using the “extRemes” and “ismev” packages within the R software programming environment (Gilleland and Katz 2006). The GEV distribution unifies a family of three continuous probability distributions and has three parameters that need to be estimated by the software algorithm: location  $\mu$ , scale  $\sigma$ ,

and a shape parameter  $\xi$  that describes the shape of the tails of the distribution. A maximum-likelihood method is used for the GEV fitting procedure, primarily because of its ease of application and its more natural association with uncertainty estimation (Gilleland et al. 2013). Once the GEV parameters have been estimated, we calculate the temperature return value, defined as the extreme maximum temperature exceeded with probability  $1/\tau$ , where  $\tau$  is the user-specified return period in years. We present all our results using  $\tau = 20$ ; that is, the 20-yr return value of maximum pavement temperature (henceforth  $TP_{\max_r20}$ ). The choice of  $\tau = 20$  produces the longest return period possible from the available observational data of 1981–2000 while not extrapolating beyond the data.

For large grids of daily data, calculating the GEV parameters can be relatively time consuming, even on modern computers: the data-processing steps for the Canada-wide GEV fitting for observations and all climate models took approximately 24 h. The GEV fitting is conducted at the native grid resolutions for observations and climate models before the return-value output data are interpolated to a common grid. The change fields are computed by first computing the difference (future minus baseline) in  $TP_{\max_r20}$  for each climate model at all grid cells and then upscaling this difference field to the observational (10 km) grid.<sup>1</sup> Next, the change fields are added to the observational  $TP_{\max_r20}$  to produce the estimates for climate change. From these estimates of  $TP_{\max_r20}$  under climate change, we compute the multimodel mean, the standard deviation, and the 25th, 50th, and 75th percentiles to represent weak, moderate, and rapid warming projections.

#### d. Conversion of air temperature to pavement temperature

The observational and model-output data provided are for maximum daily near-surface air temperature  $T_{\max}$ . We convert  $T_{\max}$  to maximum pavement temperature  $TP_{\max}$  at 20-mm depth by using the “Superpave” formula from Mills et al. [2007, their Eq. (4)]; we note that there is a typographical error in their version]:

$$TP_{\max} = a + bT_{\max} - c\phi^2 - d\log_{10}(H + e) + z(f + g\sigma_{T_{\max}}^2)^{0.5},$$

where  $\phi$  is latitude,  $H$  is the depth below the surface (mm),  $z$  is the  $z$  score corresponding to the desired

reliability [as in Mills et al. (2007), we use  $z = 2.055$  to represent a 98% reliability],  $\sigma_{T_{\max}}^2$  is the variance of the 20 annual  $T_{\max}$  values for 1981–2000, and  $a$ – $g$  are empirical (dimensionless) coefficients with respective values of 54.32, 0.78, 0.0025, 15.14, 25.0, 9.0, and 0.61. An alternative Superpave calculation for converting  $T_{\max}$  to  $TP_{\max}$  was first presented by Huber (1994) and was recently used in a study assessing the impact of climate change on asphalt-binder selection in Italy (Viola and Celauro 2015). Our tests showed that the 1994 calculation produces estimates of  $TP_{\max}$  that are systematically lower than the version used by Mills et al. (2007). For consistency with the Mills et al. report, which focused on asphalt-binder selection in Canada, we elect to retain the more recent calculation used in their report.

While various models exist for converting  $T_{\max}$  to  $TP_{\max}$ , the Superpave formula has several advantages. The Superpave system, which arose out of the Strategic Highway Research Program (SHRP), makes use of data from more than 6000 weather stations in Canada and the United States as well as long-term pavement-performance data at more than 2500 test sections located along in-service highways throughout North America. The Superpave software/formula for selecting asphalt binders was widely adopted across the United States more than a decade ago (TRB 2005). In Canada, the provinces of Ontario and Quebec completely implemented this binder specification by 2001, with other jurisdictions following in whole or in part since then (Goodman 2002). Also, there is evidence that the Superpave equations work well even in regions outside North America (e.g., Everitt 2001). For comparison, we also computed  $TP_{\max}$  using a regression equation developed by Mills et al. (2007) that was based on limited available data from stations in Ontario participating in the Ministry of Transportation’s Road Weather Information System (RWIS) project. The results using this approach (not shown) were qualitatively similar to those achieved using the Superpave method, although the RWIS-based algorithm produces a lower  $TP_{\max}$  for the same  $T_{\max}$  such that most of the cities we analyzed ended up with a category that was one pavement category below the category assigned by Superpave. Our assessment is that the Superpave formula is based on more extensive research and is used more widely across Canada, and we therefore elect to use the Superpave formula to estimate  $TP_{\max}$ .

The results presented for the change in pavement categories under climate change are constructed using annual maxima; that is, the maximum 7-day running-mean  $TP_{\max}$  value in each year, for all years in the sample (1981–2000 for baseline or 2041–70 for future). To produce Fig. 1, we also calculate  $TP_{\max}$  for each day

<sup>1</sup> This interpolation is a reasonable procedure for temperature but would be less appropriate for a variable with larger spatial variability—e.g., precipitation.



of each year, applying the conversion formula to all 7-day running-mean values of  $T_{\max}$ . This approach required using  $\sigma_{T_{\max}}^2$  (the year-to-year variance in maximum air temperature) computed over all years for each 7-day running-mean period. Although our focus here is on  $TP_{\max}$ , we note that the Superpave grading system also includes a rating for extreme *minimum* temperature, and a warming trend may reduce the potential for low-temperature cracking from extreme cold. Nevertheless, the modeling work by Mills et al. (2007) suggests that climate change may exacerbate longitudinal and alligator cracking, suggesting that diurnal and within-season variations will remain significant stressors.

### 3. Projected changes in extreme maximum pavement temperatures

#### a. Changes for major Canadian cities

Future projected changes in Canada-wide summer-time [June–August (JJA)] mean air temperature  $\Delta T_{JJA}$  are listed for each model in Table 1, along with multi-model summary statistics. The mean projected warming by 2041–70 is in the range of 1.8°–2.0°C, with the 25th percentile (a reasonable lower bound) exceeding 1.3°C and the 75th percentile (considered a conservative upper bound) well in excess of 2.0°C. This result demonstrates that all of the models display substantial warming over Canada; only one model (mri\_cgcm2\_3\_2a) projects warming below 1°C, which constitutes a similar degree of warming to that observed across North America since 1900 (Rohde et al. 2013).

Next, we address how this Canada-wide warming affects future  $TP_{\max}$ . As an example, we have calculated projected changes in  $TP_{\max}$  for the three cities shown in Fig. 1: the median GCM projection shows an increase in the extreme  $TP_{\max}$  of 0.7°, 1.8°, and 2.2°C in Vancouver, Winnipeg, and Toronto, respectively. No city shows a decrease in extreme  $TP_{\max}$ , even for the 25th-percentile model, indicating that the midcentury response to a business-as-usual-type emissions trajectory like SRES A2 is virtually certain to produce an increase in warm extremes. Last, recall that our methods assume the variance in  $TP_{\max}$  remains unchanged in a future warmer climate; any increase in temperature variability would likely lead to additional increases in the frequency of warm extremes, and evidence of this effect has been seen in modeling studies (Clark et al. 2006; Meehl and Tebaldi 2004).

Next, for our 17 selected Canadian cities we examine the projected impact of climate change on our primary metrics of interest for highway maintenance:  $TP_{\max,r20}$  and the Superpave pavement categories (the PGs). The observational baseline (1981–2000)  $TP_{\max,r20}$  for each city is indicated by the times signs in Fig. 2, and the

pavement category for the baseline period is listed in the column labeled OBS in Table 2. The majority of the cities lie within the 52°C Superpave pavement category, with Edmonton, Alberta, and St. John's, Newfoundland and Labrador, being cooler and in the 46°C category and Kelowna, British Columbia, and Windsor, Ontario, being slightly warmer and in the 58°C category. The range in projected future  $TP_{\max,r20}$  is indicated by the colored box-and-whisker plot in Fig. 2; in this section we comment only on the projections from the GCMs (pink boxes), and we return to the projections from the RCMs (blue boxes) in the next section. As expected from the projections of  $TP_{\max}$  described above, the median GCM (indicated by the black horizontal bar inside each box) shows an increase of 1°–3°C in  $TP_{\max,r20}$  for all locations; there appears to be considerable asymmetry across the country, however. Locations in interior British Columbia/Alberta (e.g., Kelowna or Calgary, Alberta) show more than 25% of the GCMs projecting decreased  $TP_{\max,r20}$ , whereas for all cities east of Thunder Bay (e.g., Toronto or Halifax, Nova Scotia) there are almost no GCMs that project decreases in  $TP_{\max,r20}$ . This pattern results from zonal asymmetries in the mean temperature response to climate change, with greater projected warming over the eastern (as compared with the western) half of North America (Maloney et al. 2014).

From an infrastructure perspective, the most important consideration is whether the Superpave category for a particular city is projected to *change* by 2041–70 (i.e., whether climate change by midcentury is likely to be associated with increased/decreased costs for pavement materials). To answer this question, we employ a threshold that is based on the projection from the median GCM: a change in PG is deemed likely when more than 50% of models project  $TP_{\max,r20}$  to be in a different category than the baseline value. On the basis of this fairly conservative criterion, 7 of 17 cities are likely to experience a change in category, covering a vast expanse of the country from Edmonton to Montreal, Quebec (50th percentile; second column from the right in Table 2). Using a more-relaxed threshold for the category change (25% of models projecting a change), the pavement category in St. John's and Regina, Saskatchewan, also changes (75th percentile; rightmost column in Table 2). We note that only in the case of Kelowna is the future pavement category projected to *decrease*, and even then only when based on projections from the 25% of GCMs showing least warming (25th percentile; third column from the right in Table 2).

#### b. Canada-wide changes in pavement category

Having examined the climatological baseline and future changes in maximum pavement temperature for

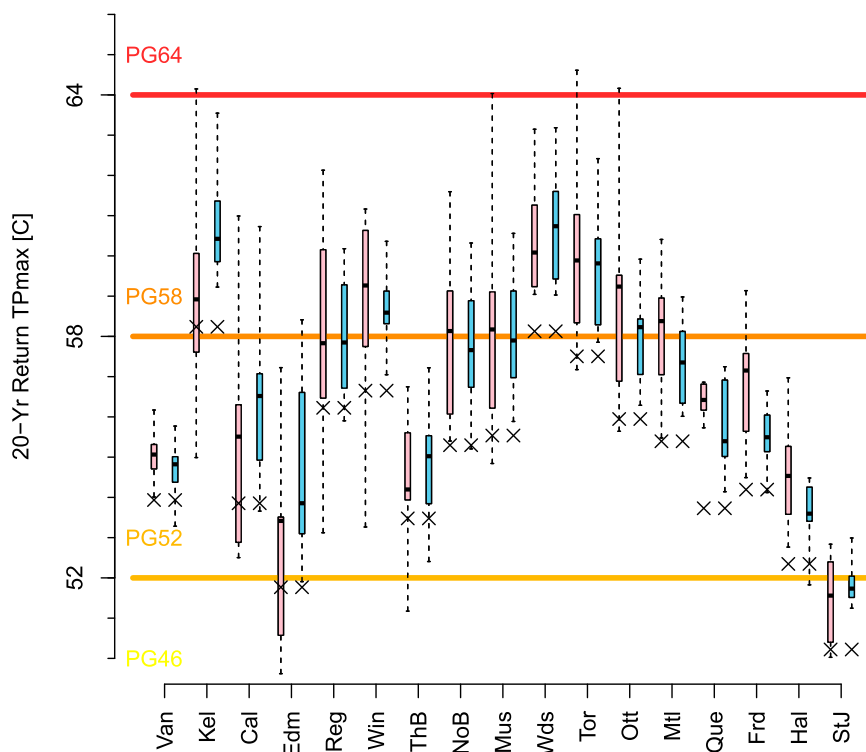


FIG. 2. Box-and-whisker plots showing ANUSPLIN baseline  $TP_{\max_r20}$  ( $^{\circ}\text{C}$ ; times signs) and GCM (pink boxes and whiskers) and RCM (blue boxes and whiskers) projected changes for 17 Canadian cities (see Table 2 for a complete list of city names). The colored horizontal lines denote the thresholds for the Superpave pavement categories (PG) at  $52^{\circ}$ ,  $58^{\circ}$ , and  $64^{\circ}\text{C}$ .

specific cities, we next turn to the spatial distribution of PG across Canada. Figure 3a shows the map of Canada-wide  $TP_{\max_r20}$  as estimated using our GEV calculation for the observational baseline period. The complex nature of extreme climate in Canada is reflected in the spatial pattern of  $TP_{\max_r20}$ : east of the Rocky Mountains it decreases roughly linearly with increasing latitude, with local variations related to large water bodies such as the Great Lakes, the Gulf of St. Lawrence, and Hudson Bay. The bulk of the Canadian population, inhabiting areas close to the southern border with the United States, resides within the  $52^{\circ}\text{C}$  pavement category. The pattern over western regions demonstrates the influence of high topography, with generally lower  $TP_{\max_r20}$  over areas of higher elevation. The majority of this region is covered by the  $46^{\circ}\text{C}$  pavement category. Figure 3a shows that for the baseline period the vast majority of Canada is covered by four main pavement categories (except for very small regions of  $58^{\circ}\text{C}$  on the shore of Lake Huron, Ontario, and in the Okanagan Valley of British Columbia).

On the basis of our calculations, that pattern is projected to change significantly in the future, with the strength of the change contingent on how much the

climate warms in response to increasing greenhouse gas concentrations. Figure 3b shows the changes in the pavement categories from some of the least sensitive model projections (the 25th percentile of all GCMs included in the analysis). Even in this weak warming case (Canada-average  $\Delta T_{\text{JJA}}$  is  $1.36^{\circ}\text{C}$ ) the area covered by the  $58^{\circ}\text{C}$  category expands into many heavily populated areas of southern Canada close to the U.S. border, where the vast majority of Canada's paved-road infrastructure is located. Farther north and west the picture is similar, showing generally northward expansion of the  $46^{\circ}$  and  $52^{\circ}\text{C}$  zones in response to a warming climate. This presents a stark conclusion: even if the actual rate of climate warming by midcentury is relatively weak, very few areas of Canada show decreases in future extreme temperatures and associated reductions in pavement category.<sup>2</sup>

<sup>2</sup> Parts of the central and western Northwest Territories are the only real exceptions, and these areas may be more susceptible to changes in wintertime minimum temperatures because of melting permafrost.

TABLE 2. The names, three-letter abbreviations (abbrev), and longitude and latitude coordinates of the 17 cities analyzed in this study. Also shown are the 20-yr return values of the Superpave PG pavement category (see section 2d) for each city for the observational (OBS) baseline period 1981–2000 and for the future period 2041–70 as based on the 25th-, 50th-, and 75th-percentile projections from the suite of GCMs following the emissions scenario SRES A2. Cities for which more than 50% of GCMs project a change in pavement category are indicated with an asterisk.

City	Abbrev	Lat (°N)	Lon (°W)	Superpave pavement category			
				OBS	GCM 25th	GCM 50th	GCM 75th
Vancouver	Van	49.2	123.1	52	52	52	52
Kelowna	Kel	49.9	119.4	58	52	58	58
Calgary	Cal	51.0	114.0	52	52	52	52
Edmonton	Edm	53.5	113.5	46	46	52*	52
Regina	Reg	50.5	104.6	52	52	52	58
Winnipeg	Win	50.0	97.2	52	52	58*	58
Thunder Bay	ThB	48.4	89.3	52	52	52	52
North Bay	NoB	46.4	78.4	52	52	58*	58
Muskoka	Mus	44.9	79.3	52	52	58*	58
Windsor	Wds	42.3	82.9	58	58	58	58
Toronto	Tor	43.7	79.6	52	58	58*	58
Ottawa	Ott	45.3	75.7	52	52	58*	58
Montreal	Mtl	45.5	73.6	52	52	58*	58
Quebec	Que	46.8	71.2	52	52	52	52
Fredericton	Frđ	46.0	66.7	52	52	52	52
Halifax	Hal	44.6	63.6	52	52	52	52
St. John's	StJ	47.6	52.7	46	46	46	52

We consider that the multi-GCM mean projected change in  $TP_{\max,r20}$  represents our “best guess” for the future spatial distribution of pavement categories (Fig. 3c). This map shows a clear and significant northward expansion of all pavement categories, with the changes considerably more widespread than for the 25th-percentile case (Fig. 3b). For example, most of southern Ontario and highly populated areas of southern Quebec shift into the 58°C category while all of northern Ontario and the majority of the prairie provinces will be in the 52°C category. We do not find any locations under this best-guess warming scenario (Canada-average  $\Delta T_{JJA}$  is 1.60°C) at which the pavement category is reduced.

For the rapid-warming case, derived from the 75th-percentile GCM projection (Fig. 3d; Canada-average  $\Delta T_{JJA}$  is 2.16°C), we see an amplified version of the multi-GCM mean pattern. The northward expansion of the 58° and 52°C categories is so pronounced that nearly all of southern Canada below 60°N is now covered by one of these two categories (the main exceptions being northeastern Quebec and higher-altitude regions of northern British Columbia). We estimate that under the scenario presented in Fig. 3d, roughly 70% of the Canadian population would be living in areas that require the 58°C pavement category (although the 52°C category covers the widest area of the country, it covers mostly sparsely populated areas). In summary, under this rapid warming scenario the majority of locations in Canada would experience a change in pavement grade,

and these changes are particularly evident in the areas of densest population and highway infrastructure.

#### 4. Examining the role of climate-model resolution

We turn next to the comparison of future projections taken from RCMs and GCMs, to see whether model horizontal resolution plays a role in the future pattern of pavement categories. The blue bars in Fig. 2 indicate the future projections of  $TP_{\max,r20}$  extracted from RCM grid cells closest to the 17 Canadian cities and can be compared with the projections from the GCMs (pink bars; see section 3a). Overall, the results from the RCMs and GCMs are similar for most locations, with the largest differences in the median projections found over interior British Columbia/Alberta, where the RCMs are warmer than the GCMs by 1°–2°C. For the spread [measured by the interquartile range (IQR)] among the different RCMs and GCMs, we find generally lower IQR for the RCMs than for the GCMs, with the notable exceptions of Edmonton and Quebec City, Quebec. An investigation of the precise cause of differences in spread is beyond the scope of this work, but it could be due to several instances in which multiple RCMs are driven by the same GCM (Table 2). This might be expected to introduce serial correlation between the output from different RCMs, which would act to reduce intermodel spread.

Even though the projected  $TP_{\max,r20}$  values are generally similar in the RCMs and GCMs, one possible source of the differences we do observe could be the



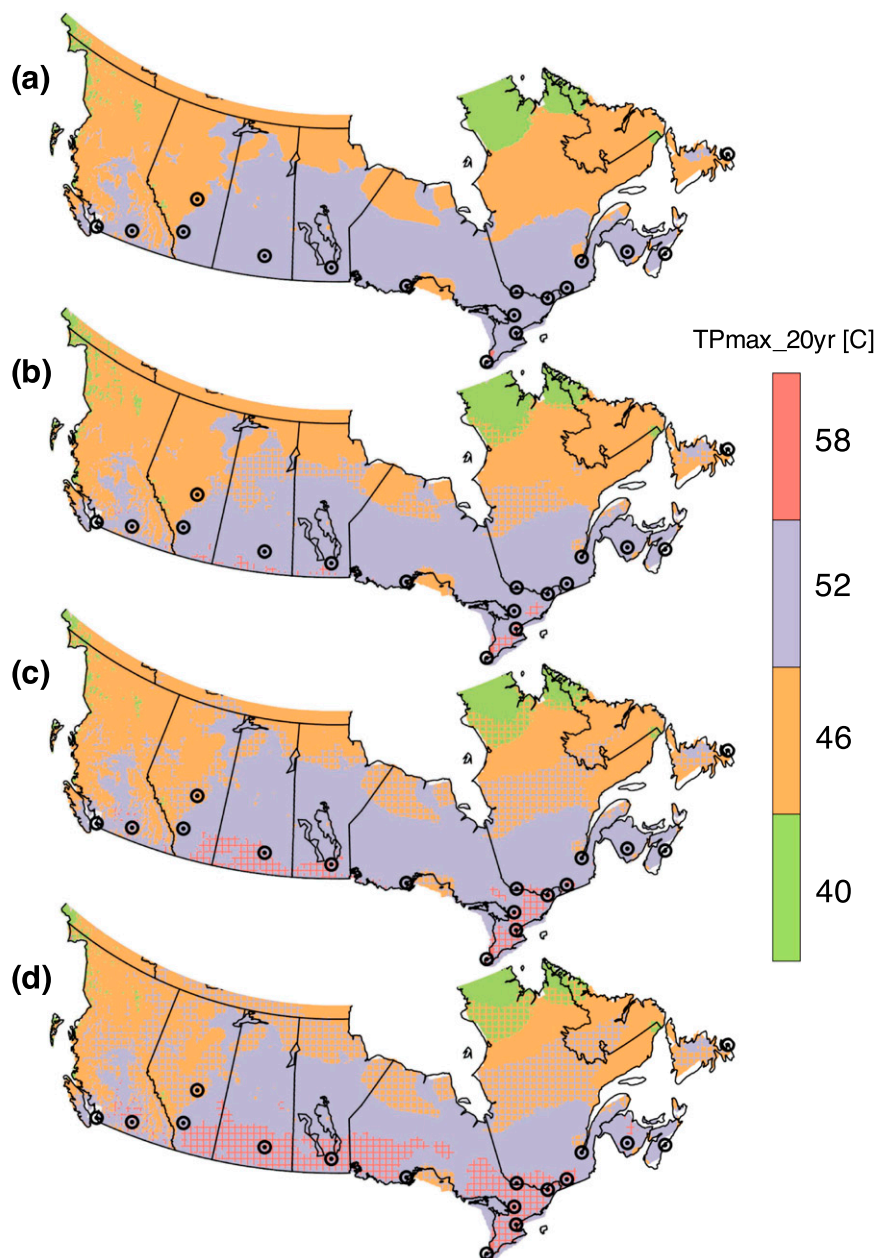


FIG. 3. The  $TP_{max\_r20}$  binned by Superpave pavement categories ( $^{\circ}\text{C}$ ). (a) The ANUSPLIN baseline 1981–2000. Also shown is the ANUSPLIN baseline from (a) but with the GCM projected  $TP_{max\_r20}$  superimposed (hatching), indicating the regions where the Superpave PG pavement category is projected to change by 2041–70, for different uncertainties derived from an ensemble of GCMs used to project future changes in extreme maximum temperature following the SRES A2 emissions scenario: (b) the 25th-percentile projected change, (c) the multi-GCM mean projected change, and (d) the 75th-percentile projected change. Dotted circles indicate the locations of the 17 cities listed in Table 2.

different rates of warming in each model, following the same SRES A2 greenhouse gas emissions scenario (i.e., the different climate sensitivities of the model ensemble). We test this effect by normalizing the projected change in  $TP_{max\_r20}$  from each model by that model's projected

$\Delta T_{JJA}$  in 2041–70. The results are shown in Fig. 4 and demonstrate better overall agreement and a reduced IQR for the GCMs and RCMs. This shift toward better agreement indicates that the ratio of city-scale temperature change to hemispheric-scale temperature change is

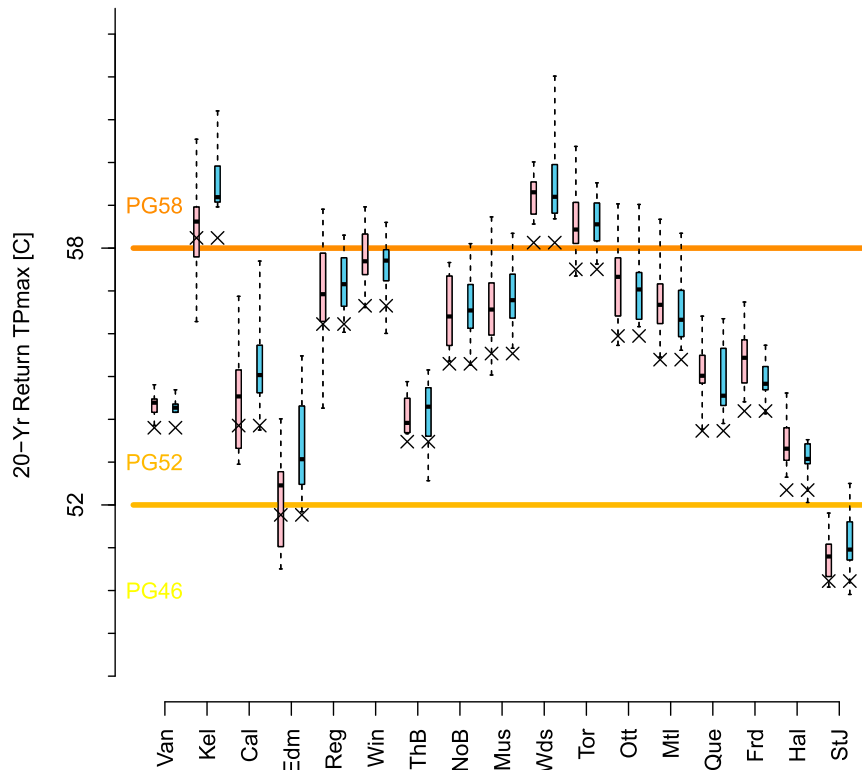


FIG. 4. As in Fig. 2, but the climate-change projections of  $TP_{\max\_r20}$  for each model (RCM or GCM) have been normalized by that model's summertime (JJA) mean Canada-wide warming. The values for the RCMs and GCMs therefore represent the change in  $TP_{\max\_r20}$  for a  $1^{\circ}\text{C}$  Canada-wide warming. The intent is to be able to compare projections of  $TP_{\max\_r20}$  between models that exhibit different levels of warming response to the same imposed climate forcing (all simulations follow the SRES A2 emissions scenario).

roughly the same in both sets of models. Note that the quantity shown for the RCMs and GCMs in Fig. 4 is the projected change in  $TP_{\max\_r20}$  for a  $1^{\circ}\text{C}$  Canada-wide  $\Delta T_{\text{JJA}}$ . Therefore, by construction, fewer cities display a change in category than we saw in Fig. 2, because most models project Canada-wide warming in excess of  $1^{\circ}\text{C}$  (Table 2). The warm bias in the RCMs seen over interior British Columbia/Alberta in Fig. 2 persists in the normalized model results (Fig. 4), suggesting that there is a real discrepancy between RCMs and GCMs in this region. The geographical location of these biases suggests strongly that high topography in the vicinity of the Rocky Mountains may play a role; we return to this point below.

Figures 5b–d show the results of our calculations superimposing the RCM-projected changes in  $TP_{\max\_r20}$  onto the baseline  $TP_{\max\_r20}$  computed from observations (note that Figs. 3a and 5a are identical). In comparing the 25th-percentile projections (Figs. 3b and 5b), it is seen that the RCMs and GCMs show very similar patterns of warming along the Canada–U.S. border, although a wider area of the southern prairie provinces is covered by the  $58^{\circ}\text{C}$  category in the RCM analysis. Similar to the GCMs,

the RCMs show a northward expansion of the  $52^{\circ}\text{C}$  zone into northern Ontario and Quebec, but the weak-warming RCM case does not produce more warming everywhere: over northern Saskatchewan and Manitoba there is a pronounced southward shift of the  $46^{\circ}\text{C}$  zone, and similar changes are found over parts of Nunavut.

For the multimodel mean projected changes that we consider to be the best guess, there is much better agreement between RCMs and GCMs (Figs. 3c and 5c). As noted for the city results, the GCMs and RCMs clearly differ over areas of high elevation in Alberta and British Columbia, which is expected since the RCMs (typical horizontal resolutions of 25–40 km) are better able to resolve high relief than the GCMs (typical horizontal resolutions of 100–200 km). For the rapid-warming 75th-percentile projection, the RCMs tend to warm slightly more everywhere than the GCMs (Figs. 3d, 5d), but both sets of models are consistent that the change in pavement categories nationwide will be profound. In broad agreement with Di Luca et al. (2013), our results indicate that, except for the differences in areas of high elevation, there is little impact on projections of extreme temperature

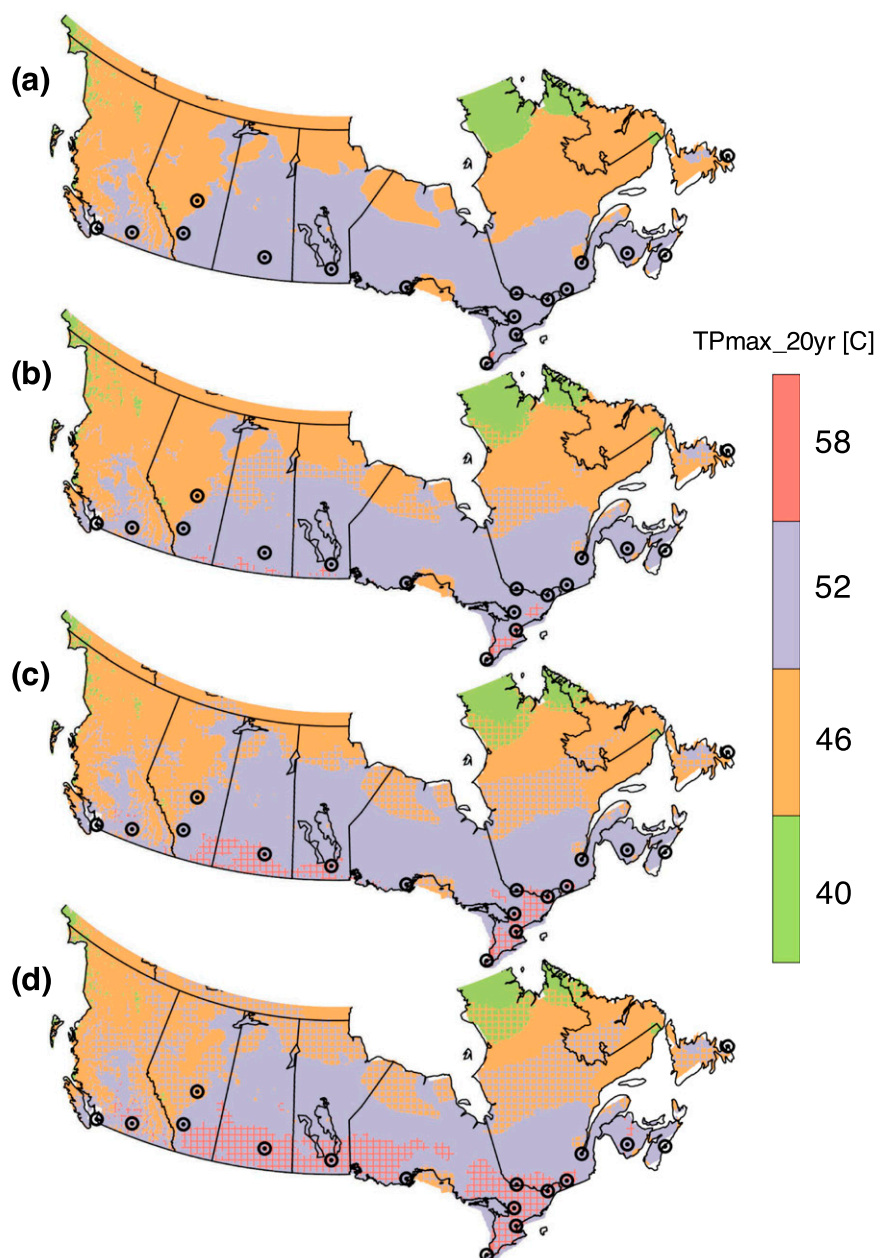


FIG. 5. As in Fig. 3 except that the projected change in  $TP_{max\_r20}$  shown in (b)–(d) is derived from the RCMs.

from using RCMs over GCMs. This finding is likely unique to temperature, however, because of its relatively homogeneous spatial distribution; previous work has shown greater added value arising from RCM simulations of precipitation (Di Luca et al. 2012).

## 5. Discussion and conclusions

This study combines climate-model output with a statistical-modeling approach to investigate mid-twenty-first-century

changes in 20-yr return values of extreme maximum pavement temperature across Canada. From the range of simulated future  $TP_{max}$ , we calculate the future performance grade for pavement for 17 major Canadian cities and assess where PG is likely to change in the future. The climate models project a range of summertime Canada-wide warming of 1°–3°C for 2041–70. As a result, all models are consistent that the change in the spatial distribution of PG nationwide will be profound, with the severity of the changes directly linked to the

severity of the projected warming. Even under weak simulated warming, an increase in PG is projected for greater Toronto, which is Canada's largest urban area, and under moderate (strong) warming 7 of 17 (9 of 17) major cities exhibit an increase. By comparing the results from global climate models with output from a set of regional climate models focused on North America, we determine that model spatial resolution is not a major determining factor for projections of future PG changes. The one region where spatial resolution does appear to be important is over mountainous terrain in western Canada.

Our methods are such that the reported changes to future extremes are very likely to be conservative. First, we assume that temperature variability will not change in the future, whereas modeling evidence indicates that variability is likely to increase under climate change (Clark et al. 2006; Tebaldi et al. 2006). Second, we elect to disregard the projections from the most extreme 50% of models (i.e., the top and bottom 25% of the ensembles), with the implicit assumption that the most likely projections will cluster around the central value. A more extreme scenario for pavement planning can be found by examining the upper tail of the model distribution (since no models project future cooling, we need not consider the lower tail). Such cases are indicated by the upper fences (whiskers) in Fig. 2, which represent  $1.5 \times \text{IQR}$ : using this metric, 12 of 17 cities exhibit a change in PG, with 3 cities in Ontario (including greater Toronto) increasing by 2 categories. Taking the projections from the individual most extreme models (data not shown) only Vancouver, Quebec City, and Halifax would have a PG that remains unchanged. Thus, the advantage of presenting a multi-model approach is that it provides planners with a full range of plausible future outcomes while simultaneously providing confidence estimates around a best guess.

Last, we comment further on our treatment of uncertainty across the model ensembles. In this analysis we present the distribution of model output (25th, 50th, and 75th percentiles) to represent equally plausible futures, and we make no attempt to differentiate between more or less accurate models. Although beyond the scope of this study, such a differentiation could prove useful in future work, since certain models have been shown to perform better at simulating summertime temperature, and several of the models within our ensembles are related (either by numerical schemes or by originating from the same institute) and thus their biases are likely to be correlated (Knutti et al. 2013; Masson and Knutti 2011). One possible method to alleviate such concerns is to calculate a weighting for each model on the basis of its fidelity in reproducing observations of a predetermined metric (e.g., summertime 7-day mean

maximum temperature) during the baseline period. Such weighting schemes are always somewhat subjective, however, and have been shown to highlight different "best" models depending on the metric used (Reichler and Kim 2008).

**Acknowledgments.** We acknowledge the modeling groups, the Program for Climate Model Diagnosis and Intercomparison (PCMDI) and the WCRP's Working Group on Coupled Modeling (WGCM), for their roles in making available the WCRP CMIP3 multimodel dataset. Authors CF and AS acknowledge funding support from an NSERC Discovery Grant and a University of Waterloo Undergraduate Research Internship.

## REFERENCES

- Boyle, J., M. Cunningham, and J. Dekens, 2013: Climate change adaptation and Canadian infrastructure: A review of the literature. International Institute for Sustainable Development Rep., 35 pp. [Available online at [http://www.redecouvrirebeton.ca/assets/files/research/Climate-Change-Adaptation-and-Canadian-Infrastructure\\_Final\\_Nov2013.pdf](http://www.redecouvrirebeton.ca/assets/files/research/Climate-Change-Adaptation-and-Canadian-Infrastructure_Final_Nov2013.pdf).]
- Chai, G., R. van Staden, H. Guan, G. Kelly, and S. Chowdhury, 2014: The impacts of climate change on pavement maintenance in Queensland, Australia. *Proc. Transport Research Arena Fifth Conf.: Transport Solutions from Research to Deployment*, Paris, France, European Commission, 10 pp. [Available online at <http://trid.trb.org/view.aspx?id=1320200>.]
- Clark, R. T., S. J. Brown, and J. M. Murphy, 2006: Modeling Northern Hemisphere summer heat extreme changes and their uncertainties using a physics ensemble of climate sensitivity experiments. *J. Climate*, **19**, 4418–4435, doi:10.1175/JCLI3877.1.
- Coles, S., 2001: *An Introduction to Statistical Modeling of Extreme Values*. Springer, 224 pp., doi:10.1007/978-1-4471-3675-0.
- Di Luca, A., R. de Elía, and R. Laprise, 2012: Potential for added value in precipitation simulated by high-resolution nested regional climate models and observations. *Climate Dyn.*, **38**, 1229–1247, doi:10.1007/s00382-011-1068-3.
- , —, and —, 2013: Potential for added value in temperature simulated by high-resolution nested RCMs in present climate and in the climate change signal. *Climate Dyn.*, **40**, 443–464, doi:10.1007/s00382-012-1384-2.
- Engineers Canada, 2008: Adapting to climate change: Canada's first national engineering vulnerability assessment of public infrastructure. Canadian Council of Professional Engineers Final Rep., 72 pp. [Available online at [http://www.pievc.ca/sites/default/files/adapting\\_to\\_climate\\_change\\_report\\_final.pdf](http://www.pievc.ca/sites/default/files/adapting_to_climate_change_report_final.pdf).]
- Everitt, P. R., 2001: Prediction of asphalt pavement temperatures in South Africa. *Proc. 20th Annual Southern African Transport Conf.*, Pretoria, South Africa, Southern African Transport Conference, 12 pp. [Available online at <http://repository.up.ac.za/handle/2263/7907>.]
- Gagnon, M., V. Gaudreault, and D. Overton, 2008: Age of public infrastructure: A provincial perspective. Statistics Canada Analysis in Brief Analytical Paper 11-621-MIE2008067, 27 pp. [Available online at <http://www.statcan.gc.ca/pub/11-621-m/11-621-m2008067-eng.pdf>.]



- Gilleland, E., and R. Katz, 2006: Analyzing seasonal to interannual extreme weather and climate variability with the extremes toolkit. *18th Conf. on Climate Variability and Change*, Atlanta, GA, Amer. Meteor. Soc., P2.15. [Available online at [https://ams.confex.com/ams/Annual2006/techprogram/paper\\_101830.htm](https://ams.confex.com/ams/Annual2006/techprogram/paper_101830.htm).]
- , M. Ribatet, and A. G. Stephenson, 2013: A software review for extreme value analysis. *Extremes*, **16**, 103–119, doi:10.1007/s10687-012-0155-0.
- Goodman, S., 2002: Superpave implementation across Canada 1994–2001: Part I. Results from the 2001 Canadian Superpave Implementation Study (C-SITS). Canadian Strategic Highway Research Program Rep., 25 pp. [Available online at <http://www.cshrp.org/products/2001C-SITSReport.PDF>.]
- Hawkins, E., and Coauthors, 2014: Uncertainties in the timing of unprecedented climates. *Nature*, **511**, E3–E5, doi:10.1038/nature13523.
- Hayhoe, K., M. Robson, J. Rogula, M. Auffhammer, N. Miller, J. VanDorn, and D. Wuebbles, 2010: An integrated framework for quantifying and valuing climate change impacts on urban energy and infrastructure: A Chicago case study. *J. Great Lakes Res.*, **36**, 94–105, doi:10.1016/j.jglr.2010.03.011.
- Hopkinson, R. F., D. W. McKenney, E. J. Milewska, M. F. Hutchinson, P. Papadopol, and L. A. Vincent, 2011: Impact of aligning climatological day on gridding daily maximum–minimum temperature and precipitation over Canada. *J. Appl. Meteor. Climatol.*, **50**, 1654–1665, doi:10.1175/2011JAMC2684.1.
- Huber, G. A., 1994: Weather database for the Superpave mix design system. National Research Council Strategic Highway Research Program Rep. SHRP-A-684A, 149 pp. [Available online at <http://onlinepubs.trb.org/onlinepubs/shrp/SHRP-A-684A.pdf>.]
- Hutchinson, M. F., D. W. McKenney, K. Lawrence, J. H. Pedlar, R. F. Hopkinson, E. Milewska, and P. Papadopol, 2009: Development and testing of Canada-wide interpolated spatial models of daily minimum–maximum temperature and precipitation for 1961–2003. *J. Appl. Meteor. Climatol.*, **48**, 725–741, doi:10.1175/2008JAMC1979.1.
- IPCC, 2014: *Climate Change 2014: Impacts, Adaptation, and Vulnerability. Part B: Regional Aspects*. V. R. Barros et al., Eds., Cambridge University Press, 688 pp. [Available online at [http://www.ipcc.ch/pdf/assessment-report/ar5/wg2/WGIIAR5-PartB\\_FINAL.pdf](http://www.ipcc.ch/pdf/assessment-report/ar5/wg2/WGIIAR5-PartB_FINAL.pdf).]
- Jaroszweski, D., E. Hooper, C. Baker, L. Chapman, and A. Quinn, 2015: The impacts of the 28 June 2012 storms on UK road and rail transport: Impacts of the 28 June 2012 storms on UK transport. *Meteor. Appl.*, **22**, 470–476, doi:10.1002/met.1477.
- Jeong, D. I., L. Sushama, G. T. Diro, M. N. Khaliq, H. Beltrami, and D. Caya, 2016: Projected changes to high temperature events for Canada based on a regional climate model ensemble. *Climate Dyn.*, doi: 10.1007/s00382-015-2759-y, in press.
- Karim, M., D. Palsat, and J. Chyc-Cies, 2014: Pavement evaluation to detect potential voids under the surface after the historic flood of June 2013 in the city of Calgary. *Proc. 2014 Conf. and Exhibition of the Transportation Association of Canada—Transportation 2014: Past, Present, Future*, Montreal, QC, Canada, Transportation Association of Canada, 18 pp. [Available online at <http://trid.trb.org/view.aspx?id=1343530>.]
- Kharin, V. V., F. W. Zwiers, and X. Zhang, 2005: Intercomparison of near-surface temperature and precipitation extremes in AMIP-2 simulations, reanalyses, and observations. *J. Climate*, **18**, 5201–5223, doi:10.1175/JCLI3597.1.
- Knutti, R., D. Masson, and A. Gettelman, 2013: Climate model genealogy: Generation CMIP5 and how we got there. *Geophys. Res. Lett.*, **40**, 1194–1199, doi:10.1002/grl.50256.
- Koerner, A., and J. Dulac, 2013: Global transport infrastructure outlook to 2050. *International Transport Forum*, Leipzig, Germany, Organization for Economic Cooperation and Development, 15 pp. [Available online at <http://www.internationaltransportforum.org/2013/pdf/koerner.pdf>.]
- Koetse, M. J., and P. Rietveld, 2009: The impact of climate change and weather on transport: An overview of empirical findings. *Transp. Res.*, **14D**, 205–221, doi:10.1016/j.trd.2008.12.004.
- Maloney, E. D., and Coauthors, 2014: North American climate in CMIP5 experiments: Part III: Assessment of twenty-first-century projections. *J. Climate*, **27**, 2230–2270, doi:10.1175/JCLI-D-13-00273.1.
- Masson, D., and R. Knutti, 2011: Climate model genealogy. *Geophys. Res. Lett.*, **38**, L08703, doi:10.1029/2011GL046864.
- McKenney, D. W., and Coauthors, 2011: Customized spatial climate models for North America. *Bull. Amer. Meteor. Soc.*, **92**, 1611–1622, doi:10.1175/2011BAMS3132.1.
- Mearns, L. O., W. Gutowski, R. Jones, R. Leung, S. McGinnis, A. Nunes, and Y. Qian, 2009: A regional climate change assessment program for North America. *Eos, Trans. Amer. Geophys. Union*, **90**, 311–311, doi:10.1029/2009EO360002.
- , and Coauthors, 2012: The North American Regional Climate Change Assessment Program: Overview of phase I results. *Bull. Amer. Meteor. Soc.*, **93**, 1337–1362, doi:10.1175/BAMS-D-11-00223.1.
- Meehl, G. A., and C. Tebaldi, 2004: More intense, more frequent, and longer lasting heat waves in the 21st century. *Science*, **305**, 994–997, doi:10.1126/science.1098704.
- Meyer, M. D., and B. Weigel, 2011: Climate change and transportation engineering: Preparing for a sustainable future. *J. Transp. Eng.*, **137**, 393–403, doi:10.1061/(ASCE)TE.1943-5436.0000108.
- Mills, B. N., S. L. Tighe, J. Andrey, J. T. Smith, S. Parm, and K. Huen, 2007: The road well-traveled: Implications of climate change for pavement infrastructure in southern Canada. Environment Canada Final Tech. Rep., 223 pp. [Available online at <http://www.bv.transports.gouv.qc.ca/mono/0970582.pdf>.]
- , —, —, —, and K. Huen, 2009: Climate change implications for flexible pavement design and performance in southern Canada. *J. Transp. Eng.*, **135**, 773–782, doi:10.1061/(ASCE)0733-947X(2009)135:10(773).
- Nakicenovic, N., and R. Swart, Eds., 2000: *Special Report on Emissions Scenarios*. Cambridge University Press, 570 pp. [Available online at [https://www.ipcc.ch/pdf/special-reports/emissions\\_scenarios.pdf](https://www.ipcc.ch/pdf/special-reports/emissions_scenarios.pdf).]
- News Staff, 2012: Toronto heat reaches record high 34.4 C on Thursday. 680 News, accessed 22 April 2015. [Available online at <http://www.680news.com/2012/06/22/toronto-heat-reaches-record-high-34-4-c-on-thursday/>.]
- Peterson, T. C., M. McGuirk, T. G. Houston, A. H. Horvitz, and M. F. Wehner, 2008: Climate variability and change with implications for transportation. National Academies Transportation Research Board Rep., 146 pp. [Available online at [http://onlinepubs.trb.org/onlinepubs/sr/sr290\\_variability.pdf](http://onlinepubs.trb.org/onlinepubs/sr/sr290_variability.pdf).]
- Regmi, M. B., and S. Hanaoka, 2011: A survey on impacts of climate change on road transport infrastructure and adaptation strategies in Asia. *Environ. Econ. Policy Stud.*, **13**, 21–41, doi:10.1007/s10018-010-0002-y.
- Reichler, T., and J. Kim, 2008: How well do coupled models simulate today's climate? *Bull. Amer. Meteor. Soc.*, **89**, 303–311, doi:10.1175/BAMS-89-3-303.



- Rohde, R., R. Muller, R. Jacobsen, S. Perlmutter, and S. Mosher, 2013: Berkeley Earth temperature averaging process. *Geoinf. Geostat.: an Overview*, **1**, doi:[10.4172/2327-4581.1000103](https://doi.org/10.4172/2327-4581.1000103).
- Seneviratne, S. I., and Coauthors, 2012: Changes in climate extremes and their impacts on the natural physical environment. *Managing the Risks of Extreme Events and Disasters to Advance Climate Change Adaptation*, C.B. Field et al., Eds., Cambridge University Press, 109–230. [Available online at [http://ipcc-wg2.gov/SREX/images/uploads/SREX-Chap3\\_FINAL.pdf](http://ipcc-wg2.gov/SREX/images/uploads/SREX-Chap3_FINAL.pdf).]
- Tebaldi, C., K. Hayhoe, J. M. Arblaster, and G. A. Meehl, 2006: Going to the extremes: An intercomparison of model-simulated historical and future changes in extreme events. *Climatic Change*, **79**, 185–211, doi:[10.1007/s10584-006-9051-4](https://doi.org/10.1007/s10584-006-9051-4).
- TRB, 2005: Superior Performing Asphalt Pavement: Superpave—Performance by design; final report of the TRB Superpave Committee. National Academies Transportation Research Board Misc. Rep., 43 pp. [Available online at <http://onlinepubs.trb.org/onlinepubs/sp/superpave.pdf>.]
- Transport Canada, 2014: Transportation in Canada 2014. Transport Canada Overview Rep., 26 pp. [Available online at [https://www.tc.gc.ca/media/documents/policy/2014\\_TC\\_Annual\\_Report\\_Overview-EN.pdf](https://www.tc.gc.ca/media/documents/policy/2014_TC_Annual_Report_Overview-EN.pdf).]
- Vincent, L. A., and É. Mekis, 2006: Changes in daily and extreme temperature and precipitation indices for Canada over the twentieth century. *Atmos.–Ocean*, **44**, 177–193, doi:[10.3137/ao.440205](https://doi.org/10.3137/ao.440205).
- Viola, F., and C. Celauro, 2015: Effect of climate change on asphalt binder selection for road construction in Italy. *Transp. Res.*, **37D**, 40–47, doi:[10.1016/j.trd.2015.04.012](https://doi.org/10.1016/j.trd.2015.04.012).
- Wuebbles, D., and Coauthors, 2014: CMIP5 climate model analyses: Climate extremes in the United States. *Bull. Amer. Meteor. Soc.*, **95**, 571–583, doi:[10.1175/BAMS-D-12-00172.1](https://doi.org/10.1175/BAMS-D-12-00172.1).
- Zhang, X., L. A. Vincent, W. D. Hogg, and A. Niitsoo, 2000: Temperature and precipitation trends in Canada during the 20th century. *Atmos.–Ocean*, **38**, 395–429, doi:[10.1080/07055900.2000.9649654](https://doi.org/10.1080/07055900.2000.9649654).